

## Calculation of Mixed Lubrication at Piston Ring and Cylinder Liner Interface

**Myung-Rae Cho,\* Jae-Kwon Choi**

*Hyundai Motor Co., Power Train Research Institute, Kyunggi-do 445-706, Korea*

**Dong-Chul Han**

*School of Mechanical and Aerospace Engineering Seoul National University,  
Seoul 151-742, Korea*

This paper reports on the theoretical analysis of mixed lubrication for the piston ring. The analytical model is presented by using the average flow and asperity contact model. The cyclic variations of the nominal minimum oil film thickness are obtained by numerical iterative method. The total friction is calculated by using the hydrodynamic and asperity contact theory. The effects of the roughness height, pattern, and engine speed on the nominal minimum film thickness, friction force, and frictional power losses are investigated. As the roughness height increases, the nominal oil film thickness and total friction force increase. Also, the effect of the surface roughness on the boundary friction is dominant at low engine speed and high asperity height. The longitudinal roughness pattern shows lower mean oil film pressure and thinner oil film thickness compared to the case of the isotropic and transverse roughness patterns.

**Key Words** : Mixed Lubrication, Piston Ring, Asperity Contact, Minimum Oil Film Thickness, Surface Roughness

### Nomenclature

$A_{ac}$  : Real contact area per unit area  
 $A_c$  : Real contact area  
 $b$  : Ring width  
 $E$  : Young's Modulus  
 $F_b$  : Boundary friction force  
 $F_c$  : Asperity contact force  
 $F_{oil}$  : Radial oil film force  
 $F_{total}$  : Total friction force  
 $F_v$  : Viscous friction force  
 $h$  : Nominal film thickness  
 $h_m$  : Nominal minimum oil film thickness  
 $h_t$  : Local oil film thickness  
 $\bar{h}_t$  : Average gap  
 $p$  : Film pressure

$p_b$  : Back pressure  
 $p_c$  : Asperity contact pressure  
 $p_{TE}$  : Elastic pressure of ring  
 $R$  : Ring radius  
 $r_c$  : Crank radius  
 $t$  : Time  
 $U$  : Sliding speed  
 $V_{r1}, V_{r2}$  : Variance ratio,  $V_{r1} = \left(\frac{\sigma_1}{\sigma}\right)^2$   
 $\alpha$  : Rate of film shear strength with pressure  
 $\beta$  : Asperity radius of curvature  
 $\delta$  : Composite roughness amplitude  
 $\gamma$  : Roughness pattern parameter  
 $\eta$  : Oil viscosity  
 $\mu$  : Asperity density  
 $\sigma$  : Composite rms roughness,  $\sigma = \sqrt{\sigma_1^2 + \sigma_2^2}$   
 $\tau_0$  : Shear strength constant  
 $\tau_v$  : Hydrodynamic component of shear stress  
 $\omega$  : Rotational speed

---

\* Corresponding Author,  
 E-mail : formell@hyundai-motor.com  
 TEL : +82-31-369-4517 ; FAX : +82-31-369-4503  
 Hyundai Motor Co., Power Train Research Institute  
 772-1 Changduk, Whasung, Kyunggi-do 445-706,  
 Korea. (Manuscript Received September 21, 2000;  
 Revised April 12, 2001)

## 1. Introduction

As fuel economy is the most important aspect of modern engine design, it is necessary to reduce the frictional power losses in the internal combustion engine. Frictional power loss from the piston ring accounts for 20–30% of the total engine frictional losses. Hence the piston ring friction is an important area of investigation.

Piston rings generally operates in the hydrodynamic lubrication regime. However, the boundary contact between the ring and liner occurs in the low speed operating mode at the TDC and BDC. The direct contact at these regime results in liner and ring wear, and leads to increased frictional losses. Therefore the proper understanding of oil film thickness on piston ring is needed to reduce the frictional losses, and to ensure engine durability.

Lloyd (1968), Ting and Mayer (1974), and Dowson, et al. (1979) performed significant hydrodynamic lubrication analysis for the piston ring. In recent years, the hydrodynamic lubrication theory has been extended to the mixed lubrication regime by combining the average Reynolds equation presented by Patir and Cheng (1978, 1979) with Greenwood and Tripp's (1971) asperity contact model. Rohde (1980) investigated ring friction and film thickness in the mixed lubrication regime and found that they depend on the surface roughness. Other studies for mixed lubrication were performed by Ping, et al. (1992), Wakuri, et al. (1995), Hamatake, et al. (1995), and Tian, et al. (1996).

In this paper, a complete one-dimensional mixed lubrication model for the piston ring is presented. The analytical model uses the average flow model for calculating the mean hydrodynamic film pressure, and asperity contact model for determining the asperity contact forces. The effects of the roughness height, patterns, and engine speed on the nominal MOFT (minimum oil film thickness), frictional force, and power losses are investigated.

## 2. Theory

### 2.1 Average Reynolds equation

The average Reynolds equation derived by Patir and Cheng (1978, 1979) is used in this study to consider the surface roughness effects. One-dimensional form of the equation is written by

$$\frac{d}{dx} \left( \frac{\phi_x h^3}{\eta} \frac{d\bar{p}}{dx} \right) = 6U \frac{d\bar{h}_t}{dx} + 6U\sigma \frac{d\phi_s}{dx} + 12 \frac{d\bar{h}_t}{dt} \quad (1)$$

In this study, a circular shape compression ring is considered, and the nominal oil film equation is expressed as follows

$$h(x, t) = h_m(t) + R(x) \quad (2)$$

In Eq. (2),  $R(x)$  is the function of the ring face profile.

Equations (3) and (4) define the local oil film thickness and the average gap.

$$h_t = h + \delta_1 + \delta_2 \quad (3)$$

$$\bar{h}_t = \int_{-h}^{\infty} (h + \delta) f(\delta) d\delta \quad (4)$$

where  $\delta$  is the composite roughness and  $f(\delta)$  the probability density function of  $\delta$  (Patir and Cheng, 1978).

By adopting the following nondimensional variables,

$$\bar{x} = \frac{x}{b}, \quad H = \frac{h}{\sigma}, \quad \bar{p} = \frac{p(\sigma/b)^2}{\eta_0 \omega}, \quad \bar{U} = \frac{U}{r_c \omega},$$

$$\tau = \omega t, \quad \phi_c = \frac{d\bar{h}}{dh}$$

Equation (1) is normalized as follows

$$\frac{d}{d\bar{x}} \left( \frac{\phi_x H^3}{\eta^*} \frac{d\bar{p}}{d\bar{x}} \right) = 6 \frac{r_c}{b} \bar{U} \left[ \phi_c \frac{dH}{d\bar{x}} + \frac{d\phi}{d\bar{x}} \right] + 12 \phi_c \frac{dH}{d\tau} \quad (5)$$

Equation (5) is solved for pressure distribution

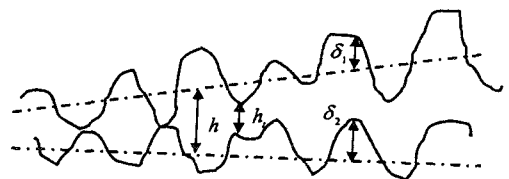


Fig. 1 Schematic diagram of surface roughness

using the classical Reynolds boundary conditions, which are given by

$$\begin{aligned} \bar{p}(-1/2) &= \bar{p}_1 \\ \bar{p}(\bar{x}_2) &= \bar{p}_2, \quad \left. \frac{\partial \bar{p}}{\partial \bar{x}} \right|_{\bar{x}_2} = 0 \end{aligned} \quad (6)$$

In Eq. (6), the boundary pressure  $\bar{p}_1$  means the cylinder pressure.

**2.2 Asperity contact model**

According to the Greenwood and Tripp's (1971) asperity contact model, the average contact pressure and contact area are expressed as follows:

$$p_c(H) = \frac{8\sqrt{2}}{15} \pi (\mu\beta\sigma)^2 E \sqrt{\frac{\sigma}{\beta}} F_{2.5}(H) \quad (7)$$

$$A_{ac}(H) = \pi^2 (\mu\beta\sigma)^2 F_2(H) \quad (8)$$

In Eqs. (7) and (8), for the surface roughness with Gaussian distributed asperity height, the function  $F_n(H)$  is defined as:

$$F_n(H) = \frac{1}{\sqrt{2\pi}} \int_H^\infty (s-H)^n e^{-\frac{s^2}{2}} ds \quad (9)$$

The asperity contact force and real contact area can be expressed as follows

$$F_c = 2\pi R \int_0^b p_c(H) dx \quad (10)$$

$$A_c = 2\pi R \int_0^b A_{ac}(H) dx \quad (11)$$

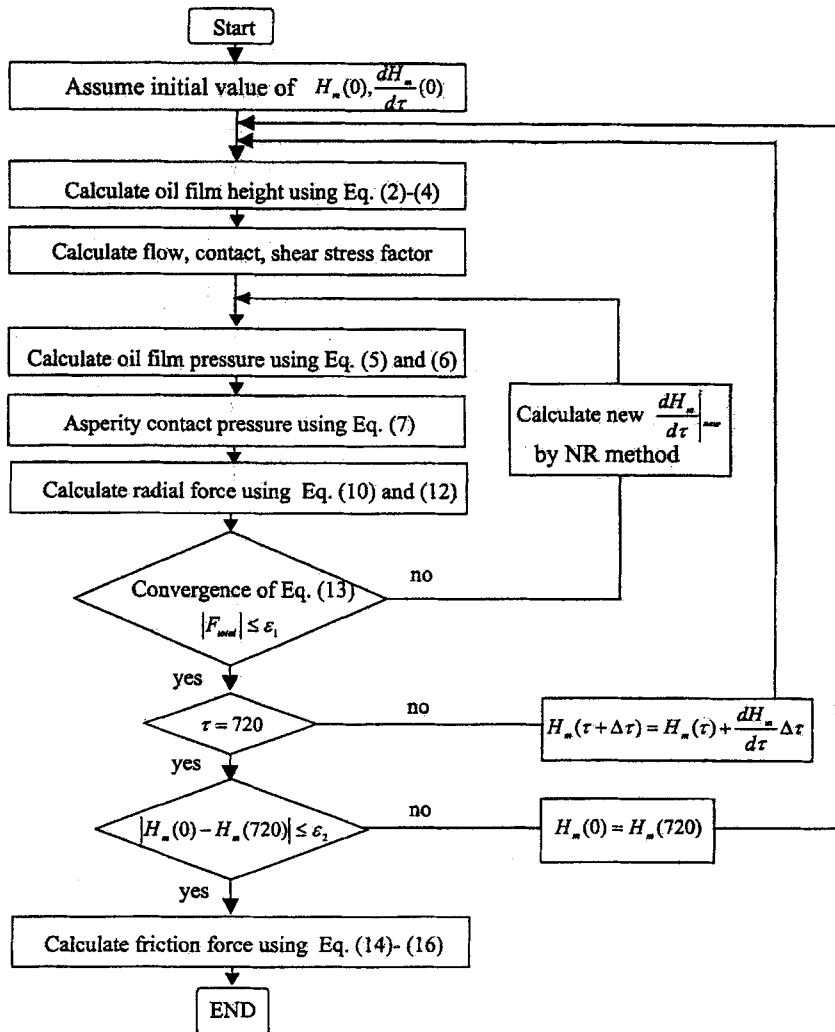


Fig. 2 Flow chart for numerical procedure

**2.3 Force equilibrium**

The radial force due to the oil film pressure can be obtained by integrating the pressure, which can be expressed as follows

$$F_{oil} = 2\pi R \int_0^b p dx \tag{12}$$

Therefore, the radial force equilibrium has the form of

$$F_{total}(H_m, \frac{dH}{dt}) = F_{oil} + F_c - 2\pi R b (p_{TE} + p_b) = 0 \tag{13}$$

In Eq. (13),  $p_b$  represents the back pressure in the piston ring, which can be obtained by the blowby analysis.

**2.4 Friction force**

The friction force between the piston ring and liner in the mixed lubrication regime consists of the viscous shearing force of the hydrodynamic oil film and boundary shearing force due to an asperity contact.

The viscous shear stress caused by the hydrodynamic lubrication is defined as follows (Patir and Cheng, 1978)

$$\tau_v = -\frac{\eta U}{h} [\phi_f + (1 - 2V_{r2})\phi_{fs}] + \frac{dp}{dx} \left[ h\phi_{fp} \left( \frac{1}{2} + V_{r2} \right) - V_{r2} \bar{h}_t \right] \tag{14}$$

and the viscous friction force can be obtained by integrating the viscous shear stress

$$F_v = 2\pi R \int_0^b \tau_v dx \tag{15}$$

The boundary friction force due to an asperity contact is written by (Rohde, 1980)

$$F_b = \tau_0 A_c + \alpha F_c \tag{16}$$

**Table 1** Specifications of the piston ring

b (mm)	2
$r_s$ (mm)	41.5
E (Gpa)	200
$\mu\beta\sigma$	0.0001
$\sigma/\beta$	0.05
$\alpha$	0.08
$\tau_0$ (MPa)	2
$\eta$ (Pa.s)	0.009

Therefore the total friction force is expressed as follows

$$F_{fric} = F_v + F_b \tag{17}$$

In the above equations, the flow factor ( $\phi_x, \phi_s$ ), contact factor ( $\phi_c$ ), and shear stress factor ( $\phi_f, \phi_{fs}, \phi_{fp}$ ) can be determined in accordance with the previous study of Patir and Cheng (1979).

Figure 2 show the numerical procedure for calculating the nominal minimum oil film thickness and friction force during an engine cycle.

**3. Results and Discussion**

Figure 3 shows the comparative result of the nominal MOFT curves between a smooth surface and a rough surface. The isotropic surface roughness pattern is used. The minimum oil film thickness of 0.36  $\mu\text{m}$  used for the smooth surface is increased to 0.58  $\mu\text{m}$  for the rough surface at the *rms* roughness of 0.8  $\mu\text{m}$ .

Figure 4 shows the effect of the roughness height on the asperity contact force, total friction force, and the nominal MOFT in the case of isotropic roughness pattern. As the *rms* roughness height increases, the MOFT increases due to the asperity interaction and stronger hydrodynamic action. In Fig. 4(b), the maximum asperity contact force occurs at the position of the minimum MOFT, corresponding to the maximum cylinder pressure position.

The asperity contact force increases as the

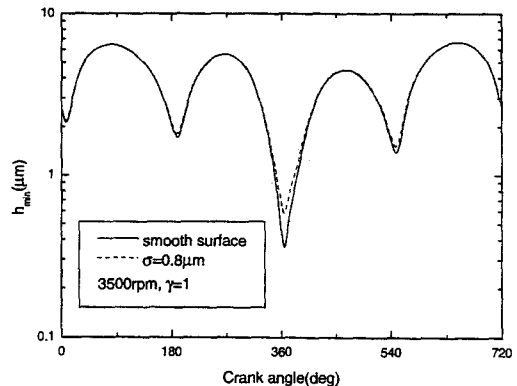
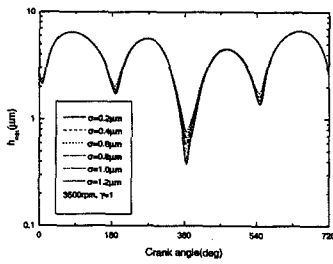


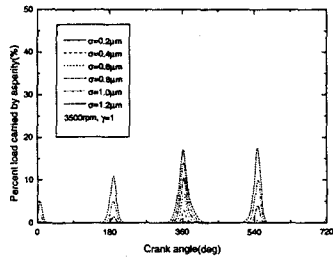
**Fig. 3** Comparative result of nominal MOFT between smooth and rough surface

roughness height increases. The hydrodynamic lubrication is dominant in the middle of the cycle due to higher sliding velocity. However, as the asperity contact occurs at the TDC and BDC area due to relatively lower sliding velocity, the boundary friction force increases at these areas (see Fig. 4(c)).

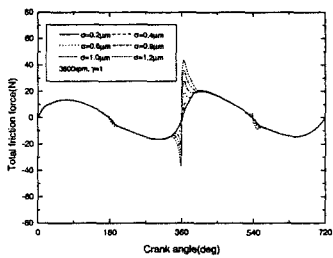
Figure 5 shows the effect of the engine speed. At higher engine speed, the nominal MOFT increases due to higher load carrying capacity of the oil film. The viscous friction force increases as the sliding velocity is increased, but the boundary friction force is reduced due to an increase in the nominal oil film thickness at high speed. The effect of the boundary friction is appeared mainly at the TDC and BDC areas, therefore, the total friction force increases as the engine speeds up.



(a) Nominal MOFT

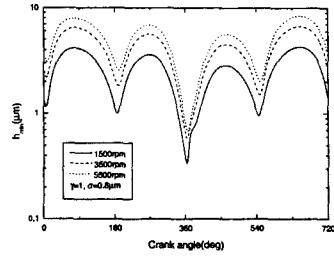


(b) Asperity contact force

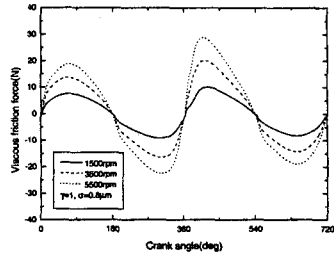


(c) Total friction force

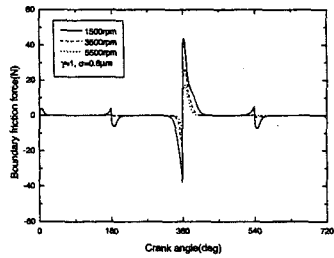
Fig. 4 The effect of roughness height



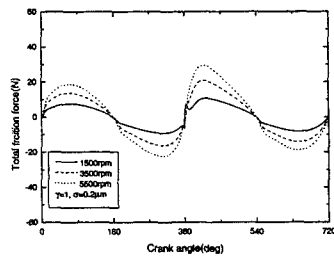
(a) Nominal MOFT



(b) Viscous friction force



(c) Boundary friction force



(d) Total friction force

Fig. 5 The effect of engine speed

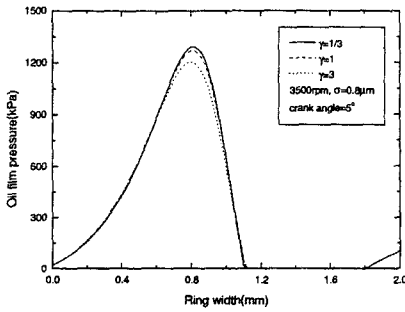
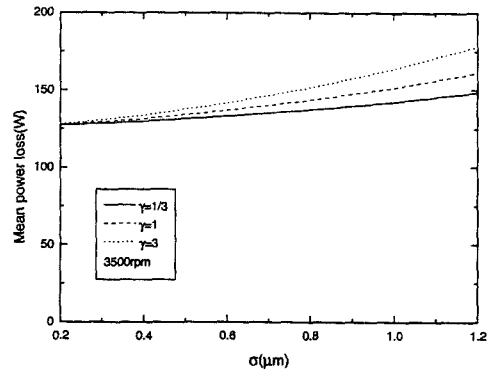
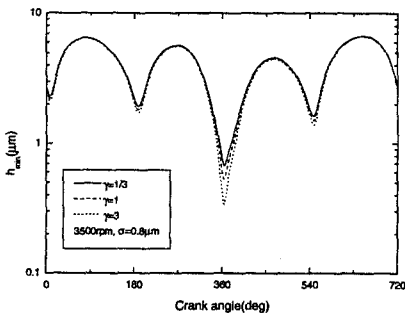


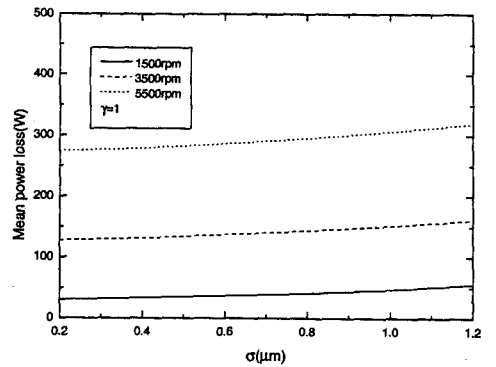
Fig. 6 The effect of surface roughness pattern on the oil film pressure at crank angle 5°



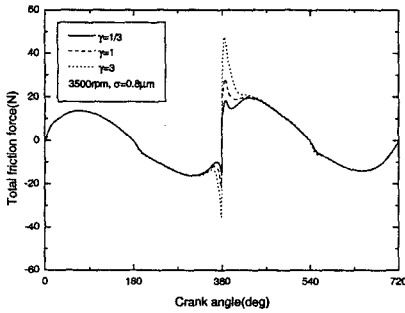
(a) Roughness pattern



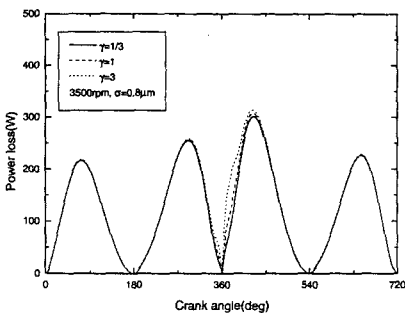
(a) Nominal MOFT



(b) Engine speed



(b) Total friction force



(c) Power loss

Fig. 7 The effect of surface roughness pattern

Fig. 8 The effect of roughness pattern and engine speed on the frictional power loss

From the above results, the effect of the asperity contact and boundary friction is dominant at low engine speed and high asperity height operating condition.

Figure 6 shows the effect of the surface roughness pattern on the mean oil film pressure. The surface roughness has three types—transverse, isotropic, and longitudinal. The transverse roughness has the maximum oil film pressure. The pressure rise and increased maximum pressure improve the radial load carrying capacity of the piston ring. Therefore, we can expect that the transverse pattern will have a thicker nominal MOFT.

Figure 7 shows the effect of the roughness pattern on the MOFT, total friction force, and frictional power loss. The transverse roughness pattern has a thicker nominal MOFT, and the maximum friction force is reduced due to a reduc-

tion of the boundary friction force and increased oil film thickness.

Figure 8 displays the effect of the roughness pattern and engine speed on the frictional power loss. As the roughness height increases, the frictional power loss increases. The power loss is increased for the longitudinal roughness pattern due to higher friction force. The effect of the roughness height on the power loss is predominant at the high asperity height region.

#### 4. Conclusions

This paper describes the mixed lubrication characteristics of the piston ring. The effects of the roughness pattern, height, and engine speed on the nominal MOFT, friction force, and power loss are investigated. The following conclusions are derived.

(1) The nominal MOFT of a rough surface is increased in comparison with a smooth surface.

(2) As the asperity height increases, the nominal MOFT, boundary friction, and power loss increases as well.

(3) As the engine speed increases, the viscous friction force increases, but the boundary friction force decreases. The total friction force is increased as the speed increases since the viscous friction is dominant during the entire engine cycle. The effect of the boundary friction is predominant at higher roughness height and lower engine speed.

(4) The transverse roughness pattern is beneficial with regard to the MOFT, friction force, and power loss.

#### References

- Dowson, D., Economou, P. N., Euddy, B. L., Strachan, P. J., and Baker, A. J. S., 1979, "Piston Ring Lubrication - Part II. Theoretical Analysis of a Single Ring and a Complete Ring Pack," *Energy Conservation Through Fluid Film Lubrication Technology: Frontiers in Research and Design*, Winter Annual Meeting of ASME, pp. 23 ~ 52.
- Greenwood, J. A., and Tripp, J. H., 1971, "The Contact of Two Nominally Flat Rough Surface," *Proc. Instn. Mech. Engrs.*, Vol. 185, 48/71.
- Hamatake, T., Wakuri, Y., Soejima, M., Kitahara, T., and Matusi, K., 1995, "Mixed Lubrication of an Oil-Control Ring in a Piston Engine", *Proc. Int. Trib. Conf.*, Yokohama, pp. 1429 ~ 1434.
- Lloyd, T., 1968, "The Hydrodynamic Lubrication of Piston Ring", *Proc. Inst. Mech. Engrs.*, Vol. 183, Part 3P, pp. 28 ~ 34.
- Patir, N., and Cheng, H. S., 1978, "An Average Flow Model for Determining Effects of Three-Dimensional Roughness on Partial Hydrodynamic Lubrication", *ASME Journal of Lubrication Technology*, Vol. 100, No. 1, pp. 12 ~ 17.
- Patir, N. and Cheng, H. S., 1979, "Application of Average Flow Model to Lubrication Between Rough Sliding Surface," *ASME Journal of Lubrication Technology*, Vol. 121, No. 2, pp. 220 ~ 230.
- Ping, C. S., and Susumu, A., 1992, "Effects of Lubricant Starvation and Surface Roughness on Piston Ring Lubrication Mechanism," *ASME. Energy-Sources Technology Conference and Exhibition*, Houston, TX.
- Rohde, S. M., 1980, "A Mixed Friction Model For Dynamically Loaded Contacts with Application to Piston Ring Lubrication," *Proc. the 7th Leeds-Lyon Symp. on Tribology*, Butterworths, pp. 262 ~ 278.
- Tian, T., Wong, V. W., and Heywood, J. B., 1996, "A Piston Ring-Pack Film Thickness and Friction Model for Multigrade Oils and Rough Surfaces," SAE962032, pp. 27 ~ 39.
- Ting, L. L., and Mayer, J. E., 1974, "Piston Ring Lubrication and Cylinder Bore Wear Analysis, Part I - Theory," *ASME Journal of Lubrication Technology*, Vol. 96, pp. 305 ~ 314.
- Wakuri, Y., Hamatake, T., Soejima, M., and Kitahara, T., 1995, "Study on the Mixed Lubrication of Piston Rings in Internal Combustion Engine," *JSME* Vol. 61, No. 538, Part C, pp. 1123 ~ 1128.